Quantum Electronics **49** (5) 493–496 (2019)

https://doi.org/10.1070/QEL16925

Tunable laser based on a semiconductor optical amplifier of red spectral region

E.V. Andreeva, A.S. Anikeev, S.N. Il'chenko, A.A. Lobintsov, A.Yu. Chamorovskii, V.R. Shidlovskii, M.V. Shramenko, S.D. Yakubovich

Abstract. **A tunable laser containing a recently developed travelling wave semiconductor optical amplifier (SOA) of the red spectral region as an active element and an acousto-optic tunable filter in an external fibre ring cavity is studied. Continuous wavelength tuning was achieved within a spectra band up to 20 nm wide with a rate up to 10^4 nm s^{-1} at a spectral linewidth below 0.04 nm and a cw output power up to 2 mW. The use of one more similar SOA as an output power amplifier made it possible to increase the output power to 15 mW.**

Keywords: *tunable laser, semiconductor optical amplifier, acousto-optic tunable filter.*

1. Introduction

Semiconductor tunable lasers operating in the red spectral region are widely used in spectroscopy, optical metrology, medicine, biology, and other fields. The photonics market offers scores of commercial models of such lasers produced by LASER 2000, TOPTICA, O/E Land, Sacher Lasertechnik, etc. (see, for example, [1, 2]). The entire tuning range of all these lasers covers the long-wavelength edge of the visible spectral region beginning from about 620 nm. As active elements of these lasers, one usually uses spatially single-mode laser diodes with antireflection-coated faces based on multilayer AlGaInP/GaInPAs nanoheterostructures of different compositions. Single-frequency lasing regime and spectral tuning are achieved by using conventional schemes of external bulk cavities containing controllable spectral-selective elements. The tuning bandwidth of individual lasers is 5–15 nm, which is determined by the optical gain bandwidth of laser diodes, which depends on the geometry and composition of their active region. The spectral linewidths of different models differ significantly, from 1 to 10^{-6} nm. As a rule, tuning is piecewise continuous. The output optical power is a few or tens of milliwatts (hundreds of milliwatts for MOPA systems).

For some practical applications, optimal lasers turned out to be BroadSweeper tunable semiconductor lasers, in which travelling wave semiconductor optical amplifiers (SOAs) are used as active elements and the radiation wavelength is controlled by an acousto-optic tunable filter (AOTF) in an external fibre cavity [3]. The tuning bands of all commercial lasers of this type together cover the wavelength range from 750 to 1100 nm [4]. The continuous tuning bandwidth of an individual laser is about 100 nm and the output optical power amounts to 20 mW. At a relatively moderate laser linewidth (~0.1 nm), these lasers have an important advantage, namely, the possibility of strictly linear emission frequency sweep in time between any two points within the tuning band with a rate up to 10^5 nm s^{-1}.

In the present work, we study a prototype of such a device for the red spectral region. To do this, it was necessary to develop corresponding SOA and AOTF and optimise necessary optical fibre components.

2. Experimental scheme

The experimental scheme is shown in Fig. 1. In principle, this scheme coincides with the MOPA system scheme described in [3]. The difference consists in the used elements. In recent works [5, 6], we reported on the creation of a series of superluminescent diodes (SLDs) for the spectral range 665–685 nm with record power characteristics. These diodes with the transverse-single-mode active channel 1400 μm long were used as amplifying elements in the developed SOAs (*1*). The modules were mounted in Butterfly housings with a Peltier microcooler and a thermistor responsible for the SOA thermostabilisation. Polarisation-maintaining PM630HP fibres with a cutoff wavelength shorter than 620 nm were used as input and output waveguides. Cylindrical microlenses at the faces of the waveguides provided a coupling coefficient of about 60%. The SOA assembling process is briefly described in [4]. The AOTF (*2*) was optimised for the optical spectral range 650–700 nm, which required deposition of corresponding antireflection coatings on the faces of the TeO_2 crystal and matching with a control generator in the frequency range 120–135 MHz. The other elements of the external ring cavity [optical isolator (*3*), fibre-optic coupler (*4*), and monitor photodiodes (*6*)] were made using the aforementioned optical fibre. Electronic controllers (*5*) and (*7*) controlled thermal stabilisation of the SOA active elements and their injection currents. Controller *5* also controlled the AOTF transmission band in manual or automatic regimes. In par-

E.V. Andreeva, S.N. Il'chenko, A.A. Lobintsov, V.R. Shidlovskii, M.V. Shramenko Opton LLC, ul. Mosfil'movskaya 17B, 119330 Moscow, Russia;
A.S. Anikeev National Research Technological University 'MISIS', Leninsky prosp. 4, 119049 Moscow, Russia;
A.Yu. Chamorovskii Superlum Diodes Ltd., Unit B3, Fota Point Enterprise Park, Carrightwohill, Co Cork, Ireland T45FC93;
S.D. Yakubovich Moscow Technological University (MIREA), prosp. Vernadskogo 78, 119454 Moscow, Russia;
e-mail: yakubovich@superlumdiodes.com

Received 3 December 2018
Kvantovaya Elektronika **49** (5) 493–496 (2019)
Translated by M.N. Basieva

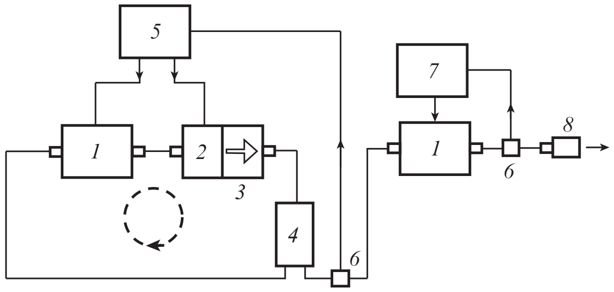

Figure 1. Optical scheme of the tunable laser with an output power amplifier (MOPA system): (*1*) SOA; (*2*) AOTF; (*3*) optical isolator; (*4*) fibre-optic coupler; (*5*) controller of the laser; (*6*) monitor photodiodes of the APC system; (*7*) controller of the output SOA; (*8*) output fibre-optic connector. Solid arrows indicate electrical connections.

ticular, it was possible to use automatic output power control (APC) upon laser wavelength tuning, including a sweep regime with a rate up to 10^4 nm s^{-1}.

Note that the considered scheme allows measuring the steady-state gain characteristics of SOAs at a narrowband input signal. For this purpose, a controlled optical attenuator and a calibrated fibre-optic coupler should be placed between the tunable laser and the SOA. Below, we present the experimental results.

3. Main physical characteristics of the tunable laser

Figure 2 presents the light–current characteristics of the laser at different frequencies of the rf control signal applied to the AOTF, which correspond to the maximum (λ = 683 nm) and the edges of the SOA gain profile. In the process of tuning, the spectral linewidth (FWHM) changes only slightly and lies within 0.034–0.039 nm (Fig. 3). The tuning curves in the APC regime at different cw output powers are presented in Fig. 4. At a power of 1 mW, the tuning range reaches 20 nm. This is obviously a record for tunable red semiconductor lasers. The measurements of the pure (fibre-to-fibre) gain of the SOA at a narrowband input signal with power $P_{\rm in}$ = 10 μW show (Fig. 5) that the gain in the range 670–690 nm exceeds 10 dB with a maximum higher than 25 dB. Figure 6 shows the SOA transmission characteristics for narrow-band input signals at wavelengths corresponding to the maximum and edges of the optical gain range. Figure 7 presents the light–current characteristics of the MOPA system in the absence of an input signal, when the SOA operates in the SLD regime, and at the

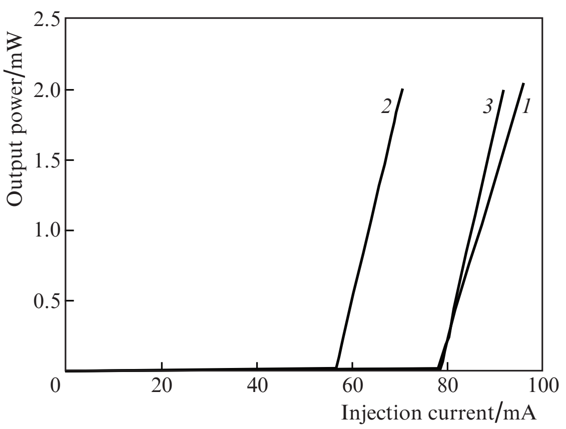

Figure 2. Light–current characteristics of the tunable laser at wavelength λ = (*1*) 673, (*2*) 683, and (*3*) 690 nm.

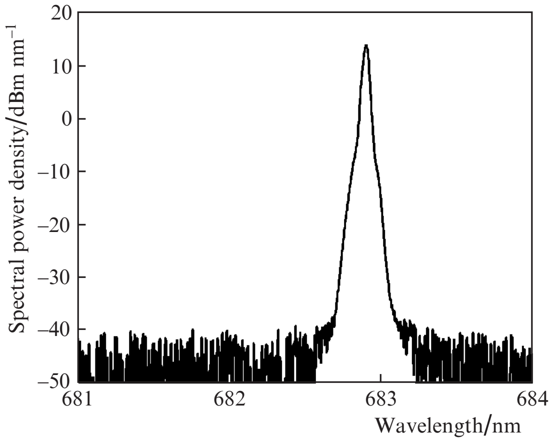

Figure 3. Output spectrum of the laser at λ = 683 nm and output power $P_{\rm out}$ = 1 mW.

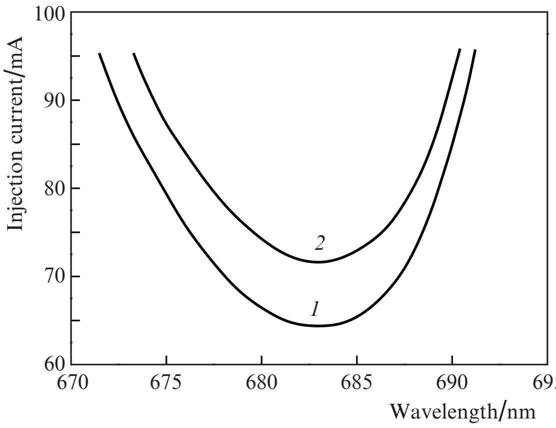

Figure 4. Tuning curves of the laser in the APC regime at output powers $P_{\rm out}$ = (*1*) 1 and (*2*) 2 mW.

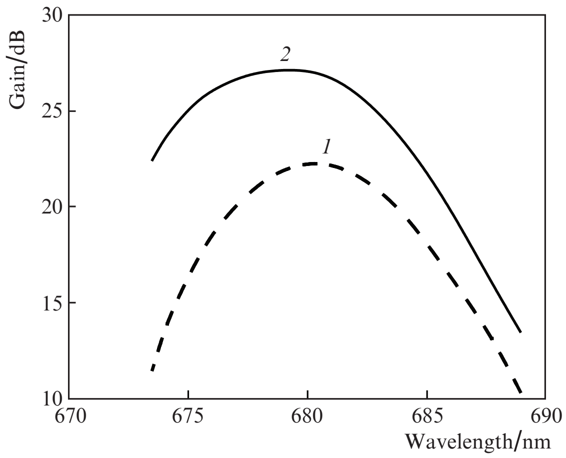

Figure 5. Small-signal gain spectrum of the SOA at injection currents of (*1*) 90 and (*2*) 125 mA.

input signal powers of 1 and 2 mW. The amplified radiation spectrum (Fig. 8) contains a superluminescent pedestal, whose height depends on the degree of optical gain saturation by the input signal. Figure 9 gives the tuning curve of the MOPA system in the APC regime at an output power of 10 mW and the corresponding dependence of the excess of the spectral brightness of the useful signal over the superluminescent background.

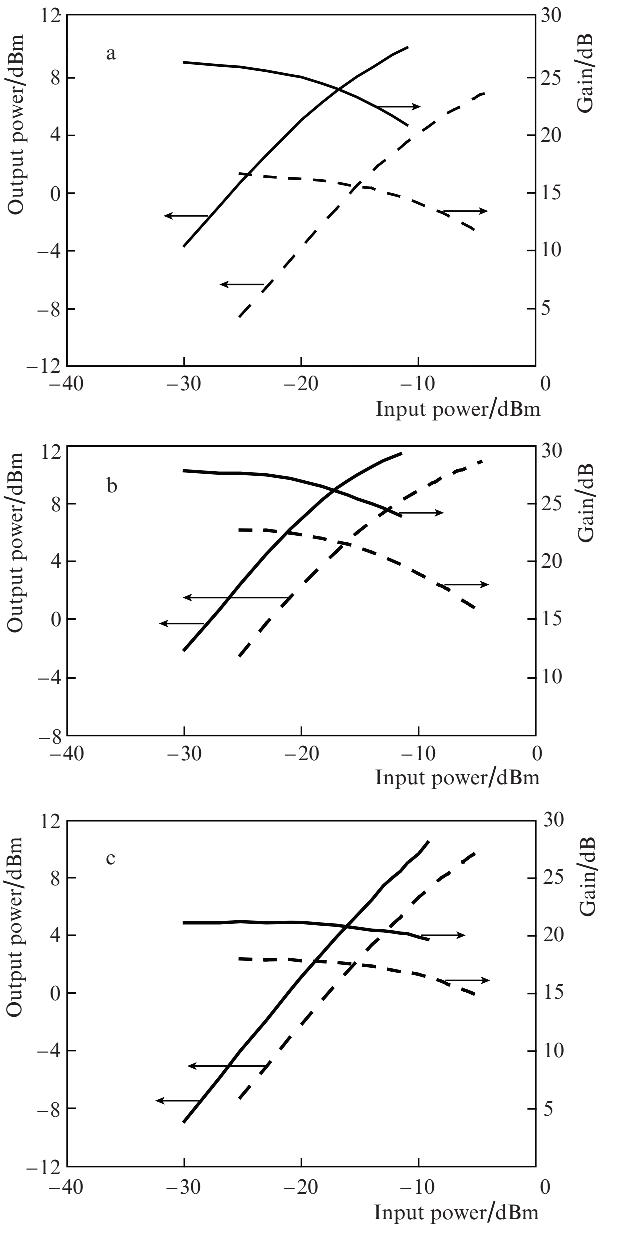

Figure 6. Transmission characteristics of the SOA for narrow-band input signals at wavelengths λ = (a) 675, (b) 680, and (c) 685 nm at injection currents of (dashed curves) 90 and (solid curves) 125 mA.

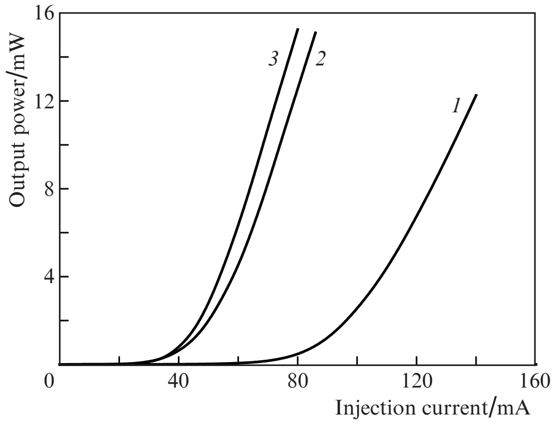

Figure 7. Light–current characteristics of the MOPA system at powers incident to the output SOA P_{in} = (*1*) 0, (*2*) 1, and (*3*) 2 mW.

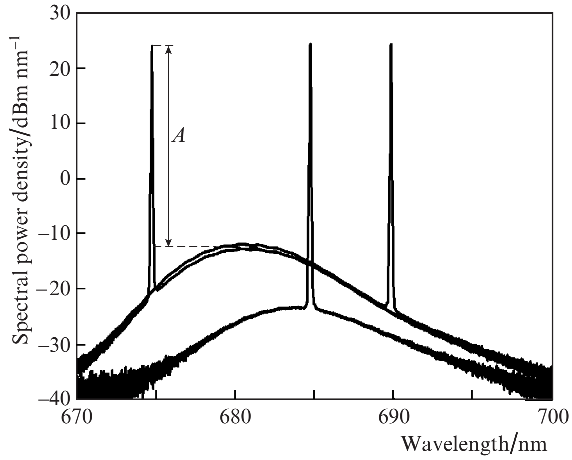

Figure 8. Output spectra of the MOPA system in the APC regime at P_{in} = 1 mW, P_{out} = 10 mW, and λ = (*1*) 675, (*2*) 683, and (*3*) 690 nm. *A* is the excess of the spectral brightness of the useful signal over the superluminescent pedestal.

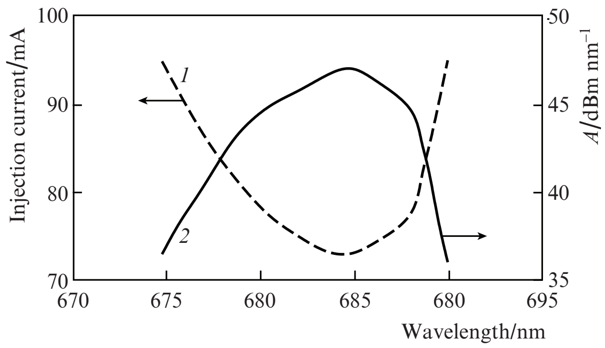

Figure 9. (*1*) Tuning curve of the MOPA system and (*2*) wavelength dependence of excess *A* of the spectral brightness of the useful signal over the superluminescent pedestal in the APC regime at P_{in} = 1 mW and P_{out} = 10 mW.

4. Conclusions

Improvement of the growth technology and post-growth processing of AlGaInP/GaInPAs nanoheterostructures made it possible to develop rather efficient and reliable SOAs of traditional configuration operating in the red spectral region and to use them for developing lasers with an AOTF in the external fibre cavity, which are tunable in the range 670–690 nm with a rate up to 10^4 nm s^{-1} at an instantaneous spectral linewidth smaller than 0.04 nm and an output power up to 15 mW.

At present, the studied devices (preliminary names SOA-262 and BS-680) are being introduced into production. We hope that these devices will find practical application in spectroscopy and optical coherence tomography, in particular, in full-field optical coherence tomography [7, 8], for which the achieved wavelength sweep rate is sufficiently high.

Acknowledgements. This work was partly supported by the Ministry of Education and Science of the Russian Federation (Project No. 8.4853.2017/BCh).

References

1. Duarte F.J. *Tunable Laser Applications* (New York: CRS press, 2016) pp 203–243.
2. www.laser2000.co.uk/lasers.php?category=5.
3. Kostin Yu.O., Ladugin M.A., Lobintsov A.A., Marmalyuk A.A., Chamorovskii A.Yu., Shramenko M.V., Yakubovich S.D. *Quantum Electron.*, **45** (8), 697 (2015) [*Kvantovaya Elektron.*, **45** (8), 697 (2015)].
4. Andreeva E.V., Il'chenko S.N., Ladugin M.A., Lobintsov A.A., Marmalyuk A.A., Shramenko M.V., Yakubovich S.D. *Quantum Electron.*, **43** (11), 994 (2013) [*Kvantovaya Elektron.*, **43** (11), 994 (2013)].
5. Andreeva E.V., Anikeev A.S., Il'chenko S.N., Chamorovsky A.Yu., Yakubovich S.D. *Electron. Lett.*, **53** (23), 1539 (2017).
6. Andreeva E.V., Anikeev A.S., Il'chenko S.N., Chamorovskii A.Yu., Yakubovich S.D. *Quantum Electron.*, **47** (12), 1154 (2017) [*Kvantovaya Elektron.*, **47** (12), 1154 (2017)].
7. Hillmann D., Franke G., Hinkel L., Bonin T., Koch P., Huttmann G. *Proc. SPIE*, **8571**, 857104 (2013).
8. Spahr H., Hillmann D., Hain C., Sudkampf H.M., Franke G., Huttmann G. *Proc. SPIE*, **9312**, 93123B (2015).